International Journal of Control and Automation
Vol.10, No.3 (2017), pp.139-160
http://dx.doi.org/10.14257/ijca.2017.10.3.12

Optimal Robust Adaptive Back-stepping Decentralized Excitation Control Based on State EKF Estimate

Zhifeng Gu[1*], Changqing Zhu[1], Guixin Yang[2] and Wenting Wang[1]

[1]*Vehicles and Electrical department, Mechanical Engineering College, Shi Jiazhuang, China;*
[2]*54th Research Institute, China Electronics Technology Corporation, Shi Jiazhuang, China*
**Email: gzfgohappy@163.com*

Abstract

This paper presents new robust adaptive L2-gain decentralized excitation controllers (C-L2-RADEC, K-L2-RADEC and OP-L2-RADEC) for the multi-machine power system. By the extended Kalman filter estimates of the state variables, the back-stepping and the linear matrix inequality method, the universal calculation formulae of the new excitation controllers are deduced. Meanwhile, the calculation of L2-gain control is simplified, and the over-parameterization problems in some adaptive methods are avoided. Simulations on a 4-machine power system demonstrate the proposed controllers can improve the robustness to disturbances, be adaptive to uncertain parameters and minimize the effect of disturbances by solving the linear matrix inequality to obtain the optimal control law.

***Keywords**: state variables estimation; optimal robust adaptive back-stepping design; optimal robust adaptive decentralized control; optimal adaptive L2 gain disturbance attenuation*

1. Introduction

In recent years, there has been an increasing interest in applying various advanced nonlinear methods in excitation to improve dynamic performance and stability of the power system [1-6]. Based on the differential geometry method, power system can be transformed into the linear models and the nonlinear control of the power system is realized by linear control methods [6]. However the exact feedback method is base on the exact knowledge of the mathematical model of the power system [7]. In order to overcome these limitations and enhance the robustness of the power system, advanced nonlinear control techniques have been used in the excitation control, such as Intelligent control [8-9], direct feedback linearization [10-11], Hamilton [12], sliding mode control [13], nonlinear robust control [14].

Because there are many disturbances and uncertain parameters in the excitation system, such as the electromagnetic interference, the torque interference and the immeasurable damping coefficient, the robust adaptive excitation control (RAEC) has attracted considerable attention [14-18]. The RAEC, using dynamic estimate of unknown parameters, is more appropriate and attractive to solve the unknown-parameter problems. Indeed, a series of literatures have discussed robust adaptive decentralized excitation control (RADEC) of the power system [3-5, 8-11, 14, 19]. However, the optimal control usually is not considered in the traditional RADEC, the over-parameterized problem exists in some robust adaptive excitation control. Moreover the values of the state variables are usually obtained by the precise sensors or encoders, which increase the system cost and complexity.

Motivated by the aforementioned observation, in this paper, the new universal robust adaptive L2-gain calculation formulas of strict parameter feedback system were deduced

ISSN: 2005-4297 IJCA

and K-class functions were used in the control law, which overcome the over-parameterized problem in some robust adaptive control and improve the convergence speed of the state parameters. Based this new L2-gain control method, new robust adaptive L2-gain decentralized excitation controllers (C-L2-RADEC, K-L2-RADEC and OP-L2-RADEC) for the power system are presented. The proposed controller is adaptive to the uncertain parameters, robust to disturbances and can be applied to minimize the impact of disturbances by solving the Linear Matrix Inequality (LMI) to obtain the optimal control law against the worst disturbances as well. In the new excitation controllers, the state parameter values of the excitation system are estimated by the extend Kalman filter (EKF).

The rest of the paper is organized as follows: in Section 2, the excitation system model of power system is established; Section 3 presents new nonlinear robust adaptive excitation controllers and the state EKF estimate; Section 4 includes the simulation results; the conclusions are summarized in Section 5.

2. Mathematical Model of Multi-machine Power System

For a large scale power system consisting of n generators interconnected through a transmission network, the model for each generator with excitation control can be written as follows [4, 10, 19-23]:

Mechanical equations:

$$\dot{\delta}_i = \omega_i - \omega_0 \tag{1.1}$$

$$\dot{\omega}_i = \frac{\omega_0}{M_i}(P_{mi} - P_{ei}) - \frac{D_i}{M_i}(\omega_i - \omega_0) + d_{i1} \tag{1.2}$$

Generator electrical dynamics:

$$\dot{E}'_{iq} = \frac{1}{T'_{d0i}}(E_{if} - E_{iq}) + \bar{d}_{i2} \tag{1.3}$$

Electrical equations:

$$E_{iq} = E'_{iq} + I_{id}(x_{id} - x'_{id}) \tag{1.4}$$

$$\delta_{ij} = \delta_i - \delta_j \tag{1.5}$$

$$P_{ie} = E'^2_{iq} G_{ii} + E'_{iq} \sum_{\substack{j=1 \\ j \neq i}}^{n} E'_{jq}(G_{ij}\cos\delta_{ij} + B_{ij}\sin\delta_{ij}) \tag{1.6}$$

$$Q_{ie} = -E'^2_{iq} B_{ii} + E'_{iq} \sum_{\substack{j=1 \\ j \neq i}}^{n} E'_{jq}(G_{ij}\sin\delta_{ij} - B_{ij}\cos\delta_{ij}) \tag{1.7}$$

$$I_{iq} = E'_{iq} G_{ii} + \sum_{\substack{j=1 \\ j \neq i}}^{n} E'_{jq}(G_{ij}\cos\delta_{ij} + B_{ij}\sin\delta_{ij}) \tag{1.8}$$

$$I_{id} = -E'_{iq} B_{ii} + \sum_{\substack{j=1 \\ j \neq i}}^{n} E'_{jq}(G_{ij}\sin\delta_{ij} - B_{ij}\cos\delta_{ij}) \tag{1.9}$$

By (1.6) and (1.8), we obtain:

$$P_{ie} = E'_{iq} I_{iq} \tag{1.10}$$

Where, δ_i is the power angle of the *i*th generator in radian; ω_i is the relative speed, in rad/s; M_i is inertia constant; P_{mi0} is the mechanical input power, assumed to be constant;

D_i is damping constant; P_{ie} is the active electrical power, in p.u.; I_{iq} is the quadrature axis current, in p.u.; $E_{iq}^{'}$ is the transient electromotive force (EMF) in the orthogonal axis of the generator, in p.u.; T'_{d0i} is the direct axis transient time constant, in *s*; I_{id} is the direct current, in p.u.; x_{id} is the direct reactance; $x_{id}^{'}$ is the transient direct reactance; will change slowly forthe saturation effect and are uncertain parameters; d_{i1} and $\bar{d}_{i2}$ are bounded model errors, represent external torque and electromagnetism disturbances, respectively; E_{fi} is EMF in the excitation coil of the generator; G_{ij} is conductance; B_{ij} is susceptance.

By (1.1)-(1.9), the excitation system of the multi-machine power system, with the uncertain parameters and the disturbances, can be rewritten as:

$$\dot{\delta}_i = \omega_i - \omega_0 \tag{2.1}$$

$$\dot{\omega}_i = (P_{mi} - P_{ei})\omega_0 / M_i - (\omega_i - \omega_0)D_i / M_i + d_{i1} \tag{2.2}$$

$$\dot{E}'_{iq} = -\frac{1}{T'_{d0i}}[E'_{iq} + I_{id}(x_{id} - x'_{id})] + \frac{1}{T'_{d0i}}E_{fi} + \bar{d}_{i2} \tag{2.3}$$

$$z_i = \left[q_{1i}(\delta_i - \delta_{i0}) \quad q_{2i}(\omega_i - \omega_0)\right]^{\mathrm{T}} \tag{2.4}$$

Where z_i is the regulation output; q_{1i} and q_{2i} are weighting constants to be determined.

Because D_i can not be measured accurately, x_{id} and $x_{id}^{'}$ usually change slowly for the saturation effect, D_i, x_{id} and $x_{id}^{'}$ are supposed as uncertain parameters.

Firstly, we introduced the following coordinate transformation:

$$\boldsymbol{x} = [x_{i1} \ \ x_{i2} \ \ x_{i3}]^{\mathrm{T}} = [\delta_i - \delta_{i0} \ \ \omega_i - \omega_{i0} \ \ \omega_{i0}(P_{mi} - P_{ei}) / M_i]^{\mathrm{T}}$$

Where δ_{i0} and ω_{i0} are the initial power angle and the rated speed of the *i*th generator, respectively.

By (1.10), we obtain:

$$\begin{aligned} \dot{x}_{i3} &= \frac{\omega_0(-\dot{E}'_{iq}I_{iq} - E'_{iq}\dot{I}_{iq})}{M_i} \\ &= \frac{-\omega_0 E'_{iq}\dot{I}_{iq}}{M_i} + \frac{-\omega_0 I_{iq}}{M_i}\{-\frac{1}{T'_{d0i}}[E'_{iq} + I_{id}(x_{id} - x'_{id})] + \frac{1}{T'_{d0i}}E_{fi} + \bar{d}_{i2}\} \\ &= v_i + \varphi_{i3}\theta_{i2} + d_{i2} \end{aligned} \tag{3}$$

Where $v_i = \frac{\omega_0}{M_i}\left[-E'_{iq}\dot{I}_{iq} + \frac{P_{ie}}{T'_{d0i}} - \frac{I_{iq}}{T'_{d0i}}E_{fi}\right]$ is the new control, $\theta_{i2} = x_{id} - x_{id}^{'}$ is the uncertain constant parameter, $\varphi_{i3} = \frac{\omega_0 I_{id} I_{iq}}{M_i T'_{d0i}}$, $d_{i2} = -\frac{\omega_0 I_{iq}}{M_i}\bar{d}_{i2}$. Obviously, d_{i2} is bounded because $\bar{d}_{i2}$ is bounded.

In the new coordinate, the excitation system of the multi-machine power system can be expressed as:

$$\dot{x}_{i1} = x_{i2} \tag{4.1}$$

$$\dot{x}_{i2} = x_{i3} - \theta_{i1}x_{i2} + d_{i1} \tag{4.2}$$

$$\dot{x}_{i3} = v_i + \varphi_{i3}\theta_{i2} + d_{i2} \quad (4.3)$$

$$\mathrm{y}_i = [q_{i1}x_{i1} \quad q_{i2}x_{i2}]^{\mathrm{T}} \quad (4.4)$$

Where $\theta_{i1} = \dfrac{D_i}{M_i}$ is uncertain constant parameter.

For System (4), the objective of the controller is to regulate E_{fi} to drive the angle δ_i and speed ω_i to a small neighborhood of a constant stable operating point. Our goal is to find $v_i = f_i(x_{i1}, x_{i2}, x_{i3})$ and $\theta_{ij} = g_{ij}(x_{i1}, x_{i2}, x_{i3})$, so that the following inequality holds:

$$\int_0^T \|\boldsymbol{y}_i\|^2 dt \le \gamma_i^2 \int_0^T \|\boldsymbol{d}_i\|^2 dt + V(\boldsymbol{x}_0) \quad (5)$$

Where $V(\boldsymbol{x}_0) \ge 0$.

Inequality (5) is the dissipative inequality of the system, which shows that the L2-gain of system (4) from disturbance $\boldsymbol{d}_i$ to output $\boldsymbol{y}_i$ is less than or equal to γ_i.

3. Design of Robust Adaptive L2-gain Decentralized Excitation Controller

3.1. New Robust Adaptive L2-gain Control Method

Excitation system (4) of power system can be considered as the special case of the following parametric strict-feedback system form:

$$\dot{x}_1 = f_1(x_1) + g_1(x_1)x_2 + \boldsymbol{\varphi}_1^{\mathrm{T}}(x_1)\boldsymbol{\theta} + \varepsilon_1 \quad (6.1)$$

$$\dot{x}_2 = f_2(x_1, x_2) + g_2(x_1, x_2)x_3 + \boldsymbol{\varphi}_2^{\mathrm{T}}(x_1, x_2)\boldsymbol{\theta} + \varepsilon_2 \quad (6.2)$$

$$\dot{x}_i = f_i(x_1,..., x_i) + g_i(x_1,..., x_i)x_{i+1} + \boldsymbol{\varphi}_i^{\mathrm{T}}(x_1,..., x_i)\boldsymbol{\theta} + \varepsilon_i \quad (6.3)$$

$$\dot{x}_n = f_n(x_1,..., x_n) + g_n(x_1,..., x_n)u + \boldsymbol{\varphi}_n^{\mathrm{T}}(x_1,..., x_n)\boldsymbol{\theta} + \varepsilon_n \quad (6.4)$$

Where $\boldsymbol{x} \in \boldsymbol{R}^n$ is the state vector; $u \in \boldsymbol{R}$ is the control input; f_i, g_i ($i = 1,2,\cdots n$) are smooth functions, $f_i(0) = 0$, $g_i(x_1,\ldots x_i) \ne 0$; $\boldsymbol{\varphi}_i(x_1,\ldots x_i)$ is smooth vector field; $\boldsymbol{\theta} \in R^p$ ($1 < p \le n$) represent unknown constant vector; ε_i ($i = 1,2,\cdots n$) is the additive disturbance in L_2 space.

Step 1: Let $e_1 = x_1$, using (6.1) to obtain:

$$\dot{e}_1 = f_1 + g_1 x_2 + \boldsymbol{\varphi}_1^{\mathrm{T}}\boldsymbol{\theta} + \varepsilon_1 \quad (7)$$

Designing the virtual control x_2^* as:

$$x_2^* = (-f_1 - \boldsymbol{\varphi}_1^{\mathrm{T}}\hat{\boldsymbol{\theta}} - m_1 e_1)/g_1 \quad (8)$$

Where $m_1 = f_1(|e_1|) + c_1 > 0$, $f_1(|e_1|)$ is the **K-**Class function, $c_1 > 0$; $\hat{\boldsymbol{\theta}}$ is the estimate value of $\boldsymbol{\theta}$; x_2^* represents the virtual control.

When $\tilde{\boldsymbol{\theta}} = \boldsymbol{\theta} - \hat{\boldsymbol{\theta}}$ and $e_2 = x_2 - x_2^*$, substituting (8) into (7) , using (6.2) and (6.1), we obtain:

$$\dot{e}_1 = -m_1 e_1 + \boldsymbol{\varphi}_1^{\mathrm{T}}\tilde{\boldsymbol{\theta}} + g_1 e_2 + \varepsilon_1 \quad (9)$$

$$\dot{e}_2 = \dot{x}_2 - \dot{x}_2^* = f_2 + g_2 x_3 + \boldsymbol{\varphi}_2^{\mathrm{T}}\boldsymbol{\theta} - \frac{\partial x_2^*}{\partial x_1}(f_1 + g_1 x_2 + \boldsymbol{\varphi}_1^{\mathrm{T}}\boldsymbol{\theta} + \varepsilon_1) - \frac{\partial x_2^*}{\partial \hat{\boldsymbol{\theta}}}\dot{\hat{\boldsymbol{\theta}}} + \varepsilon_2 \tag{10}$$

Defining Lyapunov functions as:

$$V_1 = \frac{e_1^2}{2} \tag{11}$$

$$V_2 = (e_1^2 + e_2^2)/2 \tag{12}$$

Taking the derivative of (11) and (12) along (9) and (10), yields:

$$\dot{V}_1 = -m_1 e_1^2 + e_1 \boldsymbol{\varphi}_1^{\mathrm{T}}\tilde{\boldsymbol{\theta}} + e_1 g_1 e_2 + e_1 \varepsilon_1 \tag{13}$$

$$\dot{V}_2 = -m_1 e_1^2 + e_1 \boldsymbol{\varphi}_1^{\mathrm{T}}\tilde{\boldsymbol{\theta}} + e_2 \begin{bmatrix} g_1 e_1 + f_2 + g_2 x_3 + \boldsymbol{\varphi}_2^{\mathrm{T}}\boldsymbol{\theta} - \\ \frac{\partial x_2^*}{\partial x_1}(f_1 + g_1 x_2 + \boldsymbol{\varphi}_1^{\mathrm{T}}\boldsymbol{\theta}) - \frac{\partial x_2^*}{\partial \hat{\boldsymbol{\theta}}}\dot{\hat{\boldsymbol{\theta}}} \end{bmatrix} + e_1\varepsilon_1 + e_2\varepsilon_2 - e_2\frac{\partial x_2^*}{\partial x_1}\varepsilon_1 \tag{14}$$

Designing virtual control x_3^* as:

$$x_3^* = \frac{1}{g_2}[-g_1 e_1 - f_2 - \boldsymbol{\varphi}_2^{\mathrm{T}}\hat{\boldsymbol{\theta}} + \frac{\partial x_2^*}{\partial x_1}(f_1 + g_1 x_2 + \boldsymbol{\varphi}_1^{\mathrm{T}}\hat{\boldsymbol{\theta}}) + \frac{\partial x_2^*}{\partial \hat{\boldsymbol{\theta}}}\dot{\hat{\boldsymbol{\theta}}} - m_2 e_2] \tag{15}$$

Where $m_2 = f_2(|e_2|) + c_2 > 0$, $f_2(|e_2|)$ is the **K-**Class function, $c_2 > 0$; x_3^* is the virtual control.

When $e_3 = x_3 - x_3^*$, substituting (15) into (10), (14), we obtain:

$$\dot{e}_2 = -m_2 e_2 + \boldsymbol{\varphi}_2^{\mathrm{T}}\tilde{\boldsymbol{\theta}} + g_2 e_3 - g_1 e_1 - \frac{\partial x_2^*}{\partial x_1}\boldsymbol{\varphi}_1^{\mathrm{T}}\tilde{\boldsymbol{\theta}} + \varepsilon_2 - \frac{\partial x_2^*}{\partial x_1}\varepsilon_1 \tag{16}$$

$$\dot{V}_2 = -\sum_{j=1}^{2} m_j e_j^2 + \sum_{j=1}^{2} e_j \boldsymbol{\varphi}_j^{\mathrm{T}}\tilde{\boldsymbol{\theta}} + \sum_{j=1}^{2} e_j \varepsilon_j - e_2\frac{\partial x_2^*}{\partial x_1}\boldsymbol{\varphi}_1^{\mathrm{T}}\tilde{\boldsymbol{\theta}} + g_2 e_2 e_3 - e_2\frac{\partial x_2^*}{\partial x_1}\varepsilon_1 \tag{17}$$

Step *i*:

$$V_i = \sum_{j=1}^{i}\frac{e_j^2}{2} \tag{18}$$

$$\dot{e}_i = -m_i e_i + \boldsymbol{\varphi}_i^{\mathrm{T}}\tilde{\boldsymbol{\theta}} + g_i e_{i+1} - g_{i-1}e_{i-1} - \sum_{j=1}^{i-1}\frac{\partial x_i^*}{\partial x_j}\boldsymbol{\varphi}_j^{\mathrm{T}}\tilde{\boldsymbol{\theta}} + \varepsilon_i - \sum_{j=1}^{i-1}\frac{\partial x_i^*}{\partial x_j}\varepsilon_j \tag{19}$$

$$\dot{V}_i = -\sum_{j=1}^{i} m_j e_j^2 + \sum_{j=1}^{i} e_j \boldsymbol{\varphi}_j^{\mathrm{T}}\tilde{\boldsymbol{\theta}} + \sum_{j=1}^{i} e_j\varepsilon_j - \sum_{k=2}^{i}\sum_{j=1}^{k-1} e_k\frac{\partial x_k^*}{\partial x_j}\boldsymbol{\varphi}_j^{\mathrm{T}}\tilde{\boldsymbol{\theta}} + g_i e_i e_{i+1} + \sum_{k=2}^{i}\sum_{j=1}^{k-1} e_k\frac{\partial x_k^*}{\partial x_j}\varepsilon_j \tag{20}$$

Step *n*:
Defining Lyapunov function as:

$$V_n = V_{n-1} + [f^2(e_n) + \tilde{\boldsymbol{\theta}}^{\mathrm{T}}\boldsymbol{\Gamma}^{-1}\tilde{\boldsymbol{\theta}}]/2 \tag{21}$$

Where $f(e_n)\big|_{e_n=0} \neq 0$, $\left.\frac{df(e_n)}{de_n}\right|_{e_n=0} \neq 0$.

Taking the derivative of (21), by (19) and (20), we can obtain:

$$\dot{V}_n = \dot{V}_{n-1} + f(e_n)\frac{df(e_n)}{de_n}\dot{e}_n + \tilde{\boldsymbol{\theta}}^{\mathrm{T}}\boldsymbol{\Gamma}^{-1}\dot{\tilde{\boldsymbol{\theta}}} \tag{22}$$

$$\dot{V}_n = -\sum_{j=1}^{n-1} m_j e_j^2 + \sum_{j=1}^{n-1} e_j \varepsilon_j + \sum_{j=1}^{n-1} e_j \boldsymbol{\varphi}_j^{\mathrm{T}} \tilde{\boldsymbol{\theta}} - \sum_{k=2}^{n-1}\sum_{j=1}^{k-1} e_k \frac{\partial x_{\mathrm{k}}^*}{\partial x_j} \boldsymbol{\varphi}_j^{\mathrm{T}} \tilde{\boldsymbol{\theta}} - \tilde{\boldsymbol{\theta}}^{\mathrm{T}} \boldsymbol{\Gamma}^{-1} \dot{\hat{\boldsymbol{\theta}}} - \sum_{k=2}^{n-1}\sum_{j=1}^{k-1} e_k \frac{\partial x_{\mathrm{k}}^*}{\partial x_j} \varepsilon_j + b_2[g_{n-1} e_{n-1} e_n b_2^{-1} + f_n + g_n u + \boldsymbol{\varphi}_n^{\mathrm{T}} \boldsymbol{\theta} + \varepsilon_n - \sum_{j=1}^{n-1} \frac{\partial x_n^*}{\partial x_j} (f_j + g_j x_{j+1} + \boldsymbol{\varphi}_j^{\mathrm{T}} \boldsymbol{\theta} + \varepsilon_j) - \frac{\partial x_n^*}{\partial \hat{\boldsymbol{\theta}}} \dot{\hat{\boldsymbol{\theta}}}] \tag{23}$$

Where $b_2 = f(e_n) \dfrac{df(e_n)}{de_n}$.

The nonlinear robust adaptive control law u and the adaptive law θ are as follows:

$$u = \frac{1}{g_n}\left[- g_{n-1} e_{n-1} e_n b_2^{-1} - f_n - \boldsymbol{\varphi}_n^{\mathrm{T}} \hat{\boldsymbol{\theta}} + \frac{\partial x_n^*}{\partial \hat{\boldsymbol{\theta}}} \dot{\hat{\boldsymbol{\theta}}} - m_n b_2 - u_{\mathrm{f1}} + \sum_{j=1}^{n-1} \frac{\partial x_n^*}{\partial x_j} (f_j + g_j x_{j+1} + \boldsymbol{\varphi}_j^{\mathrm{T}} \hat{\boldsymbol{\theta}}) \right] \tag{24}$$

$$\dot{\hat{\boldsymbol{\theta}}} = \left[(\sum_{j=1}^{n-1} e_j \boldsymbol{\varphi}_j^{\mathrm{T}} - \sum_{k=2}^{n-1}\sum_{j=1}^{k-1} e_k \frac{\partial x_{\mathrm{k}}^*}{\partial x_j} \boldsymbol{\varphi}_j^{\mathrm{T}} - f(e_n) \frac{df(e_n)}{de_n} \sum_{j=1}^{n-1} \frac{\partial x_n^*}{\partial x_j} \boldsymbol{\varphi}_j^{\mathrm{T}}) \boldsymbol{\Gamma} \right]^{\mathrm{T}} \tag{25}$$

Where $m_n = f_n(|e_n|) + c_n > 0$, $f_n(|e_n|)$ is the **K-**Class function, $c_n > 0$; u_{f1} is additive variable.

Substituting (24) and (25) into (23), we obtain:

$$\dot{V}_n = -\sum_{j=1}^{n-1} m_j e_j^2 - m_n b_2^2 + \sum_{j=1}^{n-1} e_j \varepsilon_j + b_2 \varepsilon_n - \sum_{k=2}^{n-1}\sum_{j=1}^{k-1} e_k \frac{\partial x_k^*}{\partial x_j} \varepsilon_j - b_2 \sum_{j=1}^{n-1} \frac{\partial x_n^*}{\partial x_j} \varepsilon_j - b_2 u_{f1} \tag{26}$$

Remark 1

By the back-stepping method, we get the following closed-loop error system:

$$\dot{e}_1 = -m_1 e_1 + \boldsymbol{\varphi}_1^{\mathrm{T}} \tilde{\boldsymbol{\theta}} + g_1 e_2 + \varepsilon_1 \tag{27.1}$$

$$\dot{e}_i = -m_i e_i + \boldsymbol{\varphi}_i^{\mathrm{T}} \tilde{\boldsymbol{\theta}} + g_i e_{i+1} - g_{i\text{-}1} e_{i\text{-}1} - \sum_{j=1}^{i-1} \frac{\partial x_i^*}{\partial x_j} \boldsymbol{\varphi}_j^{\mathrm{T}} \tilde{\boldsymbol{\theta}} + \varepsilon_i - \sum_{j=1}^{i-1} \frac{\partial x_i^*}{\partial x_j} \varepsilon_j \tag{27.i}$$

$$\dot{e}_n = -m_n e_n + u_{\mathrm{f1}} + \boldsymbol{\varphi}_n^{\mathrm{T}} \tilde{\boldsymbol{\theta}} - g_{n\text{-}1} e_{n\text{-}1} e_n b_2^{-1} - \sum_{j=1}^{n-1} \frac{\partial x_{\mathrm{n}}^*}{\partial x_j} \boldsymbol{\varphi}_j^{\mathrm{T}} \tilde{\boldsymbol{\theta}} \,\boxplus\, \varepsilon_n - \sum_{j=1}^{n-1} \frac{\partial x_{\mathrm{n}}^*}{\partial x_j} \varepsilon_j \tag{27.n}$$

$$\dot{\hat{\boldsymbol{\theta}}} = \left[(\sum_{j=1}^{n-1} e_j \boldsymbol{\varphi}_j^{\mathrm{T}} - \sum_{k=2}^{n-1}\sum_{j=1}^{k-1} e_k \frac{\partial x_{\mathrm{k}}^*}{\partial x_j} \boldsymbol{\varphi}_j^{\mathrm{T}} - f(e_n) \frac{df(e_n)}{de_n} \sum_{j=1}^{n-1} \frac{\partial x_n^*}{\partial x_j} \boldsymbol{\varphi}_j^{\mathrm{T}}) \boldsymbol{\Gamma} \right]^{\mathrm{T}} \tag{28}$$

When $\varepsilon_i = 0$, using (26), we get:

$$\dot{V}_n = -\sum_{j=1}^{n-1} m_j e_j^2 - m_n [f(e_n) \frac{df(e_n)}{dt}]^2 - b_2 u_{f1} \tag{29}$$

When $u_{\mathrm{f}1} = K b_2$ ($K > 0$), using (24) and (26), we can obtain:

$$\dot{V}_n = -\sum_{j=1}^{n-1} m_j e_j^2 - (m_n + K)\, b_2^2 \le 0 \tag{30}$$

$$u = \frac{1}{g_n}\left[- g_{n-1} e_{n-1} e_n b_2^{-1} - f_n - \boldsymbol{\varphi}_n^{T} \hat{\boldsymbol{\theta}} - (m_n + K)\, b_2 + \sum_{j=1}^{n-1} \frac{\partial x_n^*}{\partial x_j} (f_j + g_j x_{j+1} + \boldsymbol{\varphi}_j^{\mathrm{T}} \hat{\boldsymbol{\theta}}) + \frac{\partial x_n^*}{\partial \hat{\boldsymbol{\theta}}} \dot{\hat{\boldsymbol{\theta}}} \right] \tag{31}$$

Remark 2

When $f_j(|e_j|)=0$, $m_j=c_j>0$ ($j=1,2,\cdots n-\mathbf{1}$), $u_{f1}=Kf(e_n)\frac{df(e_n)}{dt}$ ($K>0$), $V_n=V_{n-1}+\frac{1}{2}f^2(e_n)+\frac{1}{2}\tilde{\boldsymbol{\theta}}^{\mathrm{T}}\boldsymbol{\Gamma}^{-1}\tilde{\boldsymbol{\theta}}\geq 0$, by $\dot{V}_n\leq 0$, we can know the closed-loop error System (27) can be stabilized by (31) and (28). Although the robust control and adaptive control of Sys (27) is realized by (31) and (28), the optimal control isn't realized.

Remark 3

When $m_j=f_j(|e_j|)+c_j$ ($j=1,2,\cdots n$), $f_j(|e_j|)$ is the **K**-class functions (for example $f_j(|e_j|)=|k_j|e_j^2$), $u_{f1}=0$, $V_n=V_{n-1}+\frac{1}{2}f^2(e_n)+\frac{1}{2}\tilde{\boldsymbol{\theta}}^{\mathrm{T}}\boldsymbol{\Gamma}^{-1}\tilde{\boldsymbol{\theta}}\geq 0$, $\dot{V}_n\leq 0$, It is same that the closed-loop error System (27) can be stabilized by (31) and (28). When the value of e_{ij} is bigger, the values of m_j and (31) will increases, so the convergence speed of System (27) will be improved.

When $\varepsilon_i\neq 0$ and the L2-gain from disturbance ε to output y of System (6) is γ, the following inequality should be hold:

$$\int_0^T\|\boldsymbol{y}\|^2dt\leq\gamma^2\int_0^T\|\boldsymbol{\varepsilon}\|^2dt+V(\boldsymbol{x}_0) \tag{32}$$

The L2-gain control of System (6) can be calculated by following methods.

Define

$$H=\dot{V}_n+\frac{1}{2}(\|\mathrm{y}(t)\|^2-\gamma^2\|\varepsilon(t)\|^2)=\dot{V}_n+\frac{1}{2}\sum_{i=1}^{n}(q_i^2x_i^2)-\frac{\gamma^2}{2}\sum_{i=1}^{n}\varepsilon_i^2 \tag{33}$$

Substituting (23) into (33), by (24) and (25), we can obtain:

$$H=-\sum_{j=1}^{n-1}m_je_j^2-m_n[f(e_n)\frac{df(e_n)}{de_n}]^2+\sum_{j=1}^{n-1}\left\{\left[e_j-\sum_{k=j+1}^{n-1}e_k\frac{\partial x_k^*}{\partial x_j}-f(e_n)\frac{df(e_n)}{de_n}\frac{\partial x_n^*}{\partial x_j}\right]\varepsilon_j-\frac{\gamma^2}{2}\varepsilon_j^2\right\}+$$
$$f(e_n)\frac{df(e_n)}{de_n}\varepsilon_n-\frac{\gamma^2}{2}\varepsilon_n^2+\frac{1}{2}\sum_{j=1}^{n}(q_jx_j)^2-f(e_n)\frac{df(e_n)}{de_n}u_{f1} \tag{34}$$

By (34), we obtain:

$$H=-\sum_{j=1}^{n-1}m_je_j^2-m_nb_2^2-\sum_{j=1}^{n-1}(\frac{\gamma\varepsilon_j}{\sqrt{2}}-\frac{b_1}{\sqrt{2}\gamma})^2+\frac{b_1^2}{2\gamma^2}-(\frac{\gamma\varepsilon_n}{\sqrt{2}}-\frac{b_2}{\sqrt{2}\gamma})^2+\frac{b_2^2}{2\gamma^2}+\frac{1}{2}\sum_{j=1}^{n}(q_jx_j)^2-b_2u_{f1} \tag{35}$$

Where $b_1=e_j-\sum_{k=j+1}^{n-1}e_k\frac{\partial x_k^*}{\partial x_j}-b_2\frac{\partial x_n^*}{\partial x_j}$.

By (35), we can obtain:

$$u_{f1}=\frac{1}{b_2}\left[\frac{b_1^2}{2\gamma^2}+\frac{b_2^2}{2\gamma^2}+\frac{1}{2}\sum_{j=1}^{n}(q_jx_j)^2\right] \tag{36}$$

By (33) and (35), yield:

$$H=-\sum_{j=1}^{n-1}m_je_j^2-m_nb_2^2-\sum_{j=1}^{n-1}(\frac{\gamma\varepsilon_j}{\sqrt{2}}-\frac{b_1}{\sqrt{2}\gamma})^2-(\frac{\gamma\varepsilon_n}{\sqrt{2}}-\frac{b_2}{\sqrt{2}\gamma})^2\leq 0 \tag{37}$$

By (37), we obtain $2\dot{V}_n\leq\gamma^2\|\varepsilon(t)\|^2-\|\mathrm{y}(t)\|^2$. Define the storage function $V(X)=2V_{\mathrm{n}}$, yield:

$$\dot{V}(X)=2\dot{V}_n\leq\gamma^2\|\boldsymbol{\varepsilon}(t)\|^2-\|\boldsymbol{y}(t)\|^2 \tag{38}$$

The integral of (38) is $V(\boldsymbol{x})-V(0)+\int_0^T\|\boldsymbol{y}\|^2dt\le\gamma^2\int_0^T\|\boldsymbol{\varepsilon}\|^2dt$. Because $V(\boldsymbol{x})=2V_n\ge 0$, we obtain $\int_0^T\|\boldsymbol{y}\|^2dt\le\gamma^2\int_0^T\|\boldsymbol{\varepsilon}\|^2dt+V(0)$. So the robust adaptive L2-gain control of System (6) can be realized by (24), (25) and (36).

Remark 4

In this paper, a new nonlinear robust adaptive L2-gain control method is proposed and the universal calculation formulas are given as (24), (25) and (36), which can reduce the calculation difficulty of the L2-gain disturbance attenuation control.

3.2. Robust Adaptive L2-gain Decentralized Excitation Control

By the method introduced in Section 3.1, the robust adaptive L2-gain decentralized excitation control can be realized by following steps:

Step 1:

$e_{i1}=x_{i1}$, $x_{i2}^*=-m_{i1}e_{i1}$ and $e_{i2}=x_{i2}-x_{i2}^*$, using (4.1) and (4.2), we obtain

$$\dot e_{i1}=\dot x_{i1}=x_{i2}=-m_{i1}e_{i1}+e_{i2} \tag{39}$$

$$\dot e_{i2}=\dot x_{i2}-\dot x_{i2}^*=x_{i3}-\theta_{i1}x_{i2}+d_{i1}+m_{i1}x_{i2} \tag{40}$$

Where $m_{i1}=f_{i1}(|e_{i1}|)+c_{i1}>0$, $f_{i1}(|e_{i1}|)$ is the **K-**Class function, $c_{i1}>0$.

Step 2:

Define $V_{i1}=\frac{e_{i1}^2}{2}$, $V_{i2}=\frac{e_{i1}^2}{2}+\frac{e_{i2}^2}{2}$. Taking the derivative of V_{i1} and V_{i2} along (39) and (40), yields:

$$\dot V_{i2}=e_{i1}\dot e_{i1}+e_{i2}\dot e_{i2}=-m_{i1}e_{i1}^2+e_{i2}(e_{i1}-\theta_{i1}x_{i2}+x_{i3}+m_{i1}x_{i2})+e_{i2}d_{i1} \tag{41}$$

Designing the stabilizing function x_3^*:

$$x_3^*=-e_{i1}+\hat\theta_{i1}x_{i2}-m_{i1}x_{i2}-m_{i2}e_{i2} \tag{42}$$

Where $m_{i2}=f_{i2}(|e_{i2}|)+c_{i2}>0$, $f_{i2}(|e_{i2}|)$ is the K-Class function, $c_{i2}>0$, $\hat\theta_{i1}$ is the estimate value of θ_{i1}.

When $e_{i3}=x_{i3}-x_{i3}^*$, by (42) and (40), we obtain

$$\dot e_{i2}=-e_{i1}-\tilde\theta_{i1}x_{i2}-m_{i2}e_{i2}+e_{i3}+d_{i1} \tag{43}$$

$$\dot e_{i3}=v_i+\varphi_{i3}\theta_{i2}+d_{i2}-m_{i1}e_{i1}+e_{i2}-\dot{\hat\theta}_{i1}x_{i2}+(-\hat\theta_{i1}+m_{i1}+m_{i2})(-\theta_{i1}x_{i2}+x_{i3}+d_{i1})+m_{i1}m_{i2}x_{i2} \tag{44}$$

$$\dot V_{i2}=e_{i1}\dot e_{i1}+e_{i2}\dot e_{i2}=-m_{i1}e_{i1}^2-m_{i2}e_{i2}^2-\tilde\theta_{i1}x_{i2}e_{i2}+e_{i2}e_{i3}+e_{i2}d_{i1} \tag{45}$$

Step 3:

Let $V_{i3}=V_{i2}+\frac{f^2(e_{i3})}{2}+\sum_{j=1}^{2}\frac{1}{2\rho_{ij}}\tilde\theta_{ij}^2$. By (45), taking derivative of V_{i3}, yields:

$$\dot V_{i3}=-m_{i1}e_{i1}^2-m_{i2}e_{i2}^2-\tilde\theta_i x_{i2}e_{i2}+e_{i2}e_{i3}+e_{i2}d_{i1}-\frac{1}{\rho_{i1}}\tilde\theta_{i1}\dot{\hat\theta}_{i1}-\frac{1}{\rho_{i2}}\tilde\theta_{i2}\dot{\hat\theta}_{i2}+b_{i2}\left(\dot x_{i3}-\dot x_{i3}^*\right) \tag{46}$$

Where $b_{i2}=f(e_{i3})df(e_{i3})/de_{i3}$.

By (42) and (4.3), we obtain:

$$\dot{V}_{i3} = -\sum_{j=1}^{2} m_{ij} e_{ij}^2 - \tilde{\theta}_{i1} x_{i2} e_{i2} + e_{i2} d_{i1} - \frac{\tilde{\theta}_{i1}\dot{\hat{\theta}}_{i1}}{\rho_{i1}} - \frac{\tilde{\theta}_{i2}\dot{\hat{\theta}}_{i2}}{\rho_{i2}} + b_{i2}\begin{bmatrix} e_{i2} e_{i3} b_{i2}^{-1} + v_i + \varphi_{i3}\theta_{i2} + d_{2i} - \\ m_{i1} e_{i1} + e_{i2} - \dot{\hat{\theta}}_{i1} x_{i2} + m_{i1} m_{i2} x_{i2} + \\ (-\hat{\theta}_{i1} + m_{i1} + m_{i2})(-\theta_{i1} x_{i2} + x_{i3} + d_{i1}) \end{bmatrix} \quad (47)$$

By (47), the control law and the adaptive law can be designed as (48), (49):

$$v_i = -e_{i2} e_{i3} b_{i2}^{-1} - \varphi_{i3}\hat{\theta}_{i2} + m_{i1}(e_{i1} - m_{i2} x_{i2}) - e_{i2} + \dot{\hat{\theta}}_{i1} x_{i2} - (-\hat{\theta}_{i1} + m_{i1} + m_{i2})(-\hat{\theta}_{i1} x_{i2} + x_{i3}) - m_{i3} b_{i2} - u_{if1} \quad (48)$$

$$\dot{\hat{\theta}}_{i1} = \rho_{i1}\left[- x_{i2} e_{i2} - (-\hat{\theta}_{i1} + m_{i1} + m_{i2}) x_{i2} b_{i2}\right] \quad (49.1)$$

$$\dot{\hat{\theta}}_{i2} = \rho_{i2} b_{i2} \varphi_{i3} \quad (49.2)$$

Where $m_{i3} = f_{i3}(|e_{i3}|) + c_{i3} > 0$, $f_{i3}(|e_{i3}|)$ is the K-Class function, $c_{i3} > 0$.
Substituting (48), (49) into (47), we obtain:

$$\dot{V}_{i3} = -\sum_{j=1}^{2} m_{ij} e_{ij}^2 - m_{i3} b_{i2}^2 - u_{if1} b_{i2} + e_{i2} d_{i1} + e_{i3} d_{i2} + b_{i2}(-\hat{\theta}_{i1} + m_{i1} + m_{i2}) d_{i1} \quad (50)$$

Substituting (48) into (44), we obtain

$$\dot{e}_{i3} = -e_{i2} e_{i3} b_{i2}^{-1} + \varphi_{i3}\tilde{\theta}_{i2} + d_{2i} - (-\hat{\theta}_i + m_{i1} + m_{i2})(\tilde{\theta}_i x_{i2} - d_{i1}) - m_{i3} b_{i2} - u_{if1} \quad (51)$$

By the back-stepping method, we obtain the following closed-loop error system

$$\dot{e}_{i1} = \dot{x}_{i1} = x_{i2} = -m_{i1} e_{i1} + e_{i2} \quad (52.1)$$

$$\dot{e}_{i2} = -e_{i1} - \tilde{\theta}_i x_{i2} - m_{i2} e_{i2} + e_{i3} + d_{i1} \quad (52.2)$$

$$\dot{e}_{i3} = -e_{i2} e_{i3} b_{i2}^{-1} + \varphi_{i3}\tilde{\theta}_{i2} + d_{2i} - (-\hat{\theta}_i + m_{i1} + m_{i2})(\tilde{\theta}_i x_{i2} - d_{i1}) - m_{i3} b_{i2} - u_{if1} \quad (52.3)$$

Define:

$$H_i = \dot{V}_{i3} + \frac{1}{2}(\|y(t)\|^2 - \gamma^2\|\varepsilon(t)\|^2) = \dot{V}_{i3} + \frac{1}{2}\sum_{j=1}^{2}(q_{ij}^2 x_{ij}^2) - \frac{\gamma^2}{2}\sum_{j=1}^{2} d_{ij}^2 \quad (53)$$

Substituting (50) into (53), we can obtain:

$$H = -\sum_{j=1}^{2} m_{ij} e_{ij}^2 - m_{i3} b_{i2}^2 - u_{if1} b_{i2} - \left(\frac{\gamma d_{i1}}{\sqrt{2}} - \frac{b_{i1}}{\sqrt{2}\gamma}\right)^2 - \left(\frac{\gamma d_{i1}}{\sqrt{2}} - \frac{e_{i3}}{\sqrt{2}\gamma}\right)^2 + \frac{b_{i1}^2}{2\gamma^2} + \frac{e_{i3}^2}{2\gamma^2} + \frac{1}{2}\sum_{j=1}^{2}(q_{ij}^2 x_{ij}^2) \quad (54)$$

Where $b_{i1} = e_{i2} + e_{i3}(-\hat{\theta}_i + m_{i1} + m_{i2})$.
By (54), we can obtain:

$$u_{if1} = \frac{1}{b_{i2}}\left[\frac{b_{i1}^2 + e_{i3}^2}{2\gamma^2} + \frac{1}{2}\sum_{j=1}^{2}(q_{ij} x_{ij})^2\right] \quad (55)$$

By (54) and (55), yield:

$$H_i = \dot{V}_{i3} + \frac{1}{2}(\|y(t)\|^2 - \gamma^2\|\varepsilon(t)\|^2) = -\sum_{j=1}^{2} m_{ij} e_{ij}^2 - m_{i3} b_{i2}^2 - \left(\frac{\gamma d_{i1}}{\sqrt{2}} - \frac{b_{i1}}{\sqrt{2}\gamma}\right)^2 - \left(\frac{\gamma d_{i1}}{\sqrt{2}} - \frac{e_{i3}}{\sqrt{2}\gamma}\right)^2 \le 0 \quad (56)$$

By (56), we obtain $2\dot{V}_{i3} \le \gamma^2\|\varepsilon(t)\|^2 - \|y(t)\|^2$. Define the storage function $V_i(X) = 2V_{i3}$, yield:

$$\dot{V}_i(X) = 2\dot{V}_{i3} \le \gamma^2\|\boldsymbol{\varepsilon}(t)\|^2 - \|\boldsymbol{y}(t)\|^2 \quad (57)$$

The integral of (57) is $V_i(\boldsymbol{x})-V_i(0)+\int_0^T\|\boldsymbol{y}\|^2dt\le\gamma^2\int_0^T\|\boldsymbol{\varepsilon}\|^2dt$. Because $V_i(\boldsymbol{x})=2V_{i3}\ge 0$, we obtain $\int_0^T\|\boldsymbol{y}\|^2dt\le\gamma^2\int_0^T\|\boldsymbol{\varepsilon}\|^2dt+V_i(0)$. So the robust adaptive L2-gain control of excitation system (4) can be realized by (48), (49) and (55).

Remark 5

The robust adaptive L2-gain controller of excitation system (4) can be realized by (48), (49) and (55). When $m_{ij}=c_{ij}$ and $f_{ij}(|e_{ij}|)=0$ (j=1, 2, 3), this controller can be called constant-L2-gain-robust-adaptive-decentralized-excitation-controller (C-L2-RADEC). When $f_{ij}(|e_{ij}|)\neq 0$ (*j*=1, 2, 3), this controller can be called K-class-function-L2-gain-robust-adaptive-decentralized-excitation-controller (K-L2-RADEC). When the values of e_{ij} are bigger, the value of $m_{ij}=f(|e_{ij}|)+c_{ij}=|k_{ij}|e_{ij}^2+c_{ij}$ will increase, so this K-L2-RADEC will improve the control speed. However, the optimal excitation control isn't considered in C-L2-RADEC and K-L2-RADEC. In Section 3.3, a new optimal K-class-function-L2-gain-robust-adaptive-decentralized-excitation-controller (OP-L2-RADEC) will be introduced.

3.3. Optimal Robust Adaptive L2-gain Decentralized Excitation Control

If $V_{i3}=V_{i2}+\dfrac{e_{i3}^2}{2}+\sum_{j=1}^{2}\dfrac{1}{2\rho_{ij}}\tilde{\theta}_{ij}^2$, by (39)-(45), we will obtain:

$$\dot{V}_{i3}=-m_{i1}e_{i1}^2-m_{i2}e_{i2}^2-\tilde{\theta}_{i1}x_{i2}e_{i2}+e_{i2}e_{i3}+e_{i2}d_{i1}-\frac{\tilde{\theta}_{i1}\dot{\hat{\theta}}_{i1}}{\rho_{i1}}-\frac{\tilde{\theta}_{i2}\dot{\hat{\theta}}_{i2}}{\rho_{i2}}+e_{i3}\left(\dot{x}_{i3}-\dot{x}_{i3}^*\right) \tag{58}$$

By (40) and (4.3), we obtain:

$$\dot{V}_{i3}=-\sum_{j=1}^{2}m_{ij}e_{ij}^2-\tilde{\theta}_{i1}x_{i2}e_{i2}+e_{i2}d_{i1}-\frac{\tilde{\theta}_{i1}\dot{\hat{\theta}}_{i1}}{\rho_{i1}}-\frac{\tilde{\theta}_{i2}\dot{\hat{\theta}}_{i2}}{\rho_{i2}}+e_{i3}\begin{bmatrix}e_{i2}+v_i+\varphi_{i3}\theta_{i2}+d_{2i}-m_{i1}e_{i1}+e_{i2}+\\(-\hat{\theta}_{i1}+m_{i1}+m_{i2})(-\theta_{i1}x_{i2}+x_{i3}+d_{i1})+\\m_{i1}m_{i2}x_{i2}-\dot{\hat{\theta}}_{i1}x_{i2}\end{bmatrix} \tag{59}$$

By (59), the control law and the adaptive law can be designed as (60), (61), respectively:

$$\begin{aligned}v_i=&-e_{i2}+m_{i1}e_{i1}-e_{i2}-\varphi_{i3}\hat{\theta}_{i2}+\dot{\hat{\theta}}_i x_{i2}-m_{i1}m_{i2}x_{i2}\\&-(-\hat{\theta}_i+m_{i1}+m_{i2})(-\hat{\theta}_i x_{i2}+x_{i3})-m_{i3}e_{i3}-u_{if1}\end{aligned} \tag{60}$$

$$\dot{\hat{\theta}}_{i1}=\rho_{i1}\left[-x_{i2}e_{i2}-(-\hat{\theta}_{i1}+m_{i1}+m_{i2})x_{i2}e_{i3}\right] \tag{61.1}$$

$$\dot{\hat{\theta}}_{i2}=\rho_{i2}e_{i3}\varphi_{i3} \tag{61.2}$$

Where $m_{i3}=f_{i3}(|e_{i3}|)+c_{i3}>0$, $f_{i3}(|e_{i3}|)$ is the K-Class function, $c_{i3}>0$.

Substituting (60) into (44), we obtain

$$\dot{e}_{i3}=-e_{i2}+\varphi_{i3}\tilde{\theta}_{i2}+d_{2i}-(-\hat{\theta}_i+m_{i1}+m_{i2})(\tilde{\theta}_i x_{i2}-d_{i1})-m_{i3}e_{i3}-u_{if1} \tag{62}$$

We obtain the following closed-loop error system:

$$\dot{e}_{i1}=\dot{x}_{i1}=x_{i2}=-m_{i1}e_{i1}+e_{i2} \tag{63.1}$$

$$\dot{e}_{i2}=-e_{i1}-\tilde{\theta}_{i1}x_{i2}-m_{i2}e_{i2}+e_{i3}+d_{i1} \tag{63.2}$$

$$\dot{e}_{i3} = -e_{i2} + \varphi_{i3}\tilde{\theta}_{i2} + d_{2i} - \left(-\hat{\theta}_i + m_{i1} + m_{i2}\right)\tilde{\theta}_i x_{i2} - m_{i3}e_{i3} + \left(-\hat{\theta}_i + m_{i1} + m_{i2}\right)d_{i1} - u_{if1} \quad (63.3)$$

By (63), we obtain:

$$\dot{z}_{i1} = z_{i2} = \dot{e}_{i1} = -m_{i1}e_{i1} + e_{i2} \quad (64.1)$$

$$\dot{z}_{i2} = -m_{i1}\dot{e}_{i1} + \dot{e}_{i2} = \left(m_{i1}^2 - 1\right)e_{i1} - \left(m_{i1} + m_{i2}\right)e_{i2} + e_{i3} - \tilde{\theta}_{i1}x_{i2} + d_{i1} = z_{i3} + \varepsilon_{i1} \quad (64.2)$$

$$\begin{aligned}\dot{z}_{i3} &= \dot{\hat{\theta}}_{i1}x_{i2} + \hat{\theta}_{i1}\dot{x}_{i2} + \left(m_{i1}^2 - 1\right)\dot{e}_1 - \left(m_{i1} + m_{i2}\right)\dot{e}_{i2} + \dot{e}_{i3} \\ &= (-m_{i1}^3 + 2m_{i1} + m_{i2})z_{i1} + \bar{v}_{i1} + \varepsilon_{i2}\end{aligned} \quad (64.3)$$

$$\bar{v}_{i1} = \left(m_{i1}^2 + m_{i2}^2 + m_{i1}m_{i2} - 2\right)e_{i2} - u_{if1} - \left(m_{i1} + m_{i2} + m_{i3}\right)e_{i3} + \dot{\hat{\theta}}_{i1}x_{i2} \quad (64.4)$$

Where $z_{i1} = \delta_i - \delta_{i0}$; $z_{i2} = \omega_i - \omega_{i0}$; $z_{i3} = \dot{\omega}_i$, $\varepsilon_{i1} = d_{i1}$; $\varepsilon_{i2} = \tilde{\theta}_{i1}(\hat{\theta}_{i1}x_{i2} - \dot{x}_{i2}) + \varphi_{i3}\tilde{\theta}_{i2} - \hat{\theta}_{i1}d_{i1} + d_{i2}$; d_{i1}, d_{i2}, θ_{i1}, θ_{i2} and x_{i2} are in L2-space; $\varepsilon_{i1} \in L_2$ and $\varepsilon_{i2} \in L_2$.

By (64), we can obtain the state equation:

$$\begin{aligned}\dot{\boldsymbol{Z}}_i = \begin{bmatrix}\dot{z}_{i1} \\ \dot{z}_{i2} \\ \dot{z}_{i3}\end{bmatrix} &= \begin{bmatrix}0 & 1 & 0 \\ 0 & 0 & 1 \\ -m_{i1}^3 + 2m_{i1} + m_{i2} & 0 & 0\end{bmatrix}\begin{bmatrix}z_{i1} \\ z_{i2} \\ z_{i3}\end{bmatrix} + \begin{bmatrix}0 & 0 \\ 1 & 0 \\ 0 & -1\end{bmatrix}\begin{bmatrix}\varepsilon_{i1} \\ \varepsilon_{i2}\end{bmatrix} + \begin{bmatrix}0 \\ 0 \\ 1\end{bmatrix}\bar{v}_{i1} \\ &= \boldsymbol{A}_i\boldsymbol{Z}_i + \boldsymbol{B}_{i1}\boldsymbol{\varepsilon}_i + \boldsymbol{B}_{i2}\bar{v}_{i1}\end{aligned} \quad (65)$$

Theorem 1

When $\boldsymbol{y}_i = \boldsymbol{C}_i\boldsymbol{Z}_i$, if the minimum value of γ_i ($\gamma_i > 0$) can be found and System (64) satisfies $\int_0^T \|\boldsymbol{y}_i\|^2 dt \le \gamma_i^2 \int_0^T (\|\boldsymbol{w}_i\|^2) dt$ ($T > 0$), the optimal L2-gain control of System (64) is realized and the L2-gain will be less than or equal to γ_i. The optimal control law and the worst disturbance are as follows:

$$\bar{v}_{i1} = \boldsymbol{W}_i\boldsymbol{P}_i^{-1}\boldsymbol{Z}_i \quad (66)$$

$$\boldsymbol{\varepsilon}_i = \frac{1}{\gamma_i^2}\boldsymbol{B}_{i1}^{\mathrm{T}}\boldsymbol{P}_i^{-1}\boldsymbol{Z}_i \quad (67)$$

Where $\boldsymbol{W}_i$ and $\boldsymbol{P}_i$ are the solutions of the following linear matrix inequality (68).

$$\begin{bmatrix}(\boldsymbol{A}_i + \boldsymbol{B}_{i2}\boldsymbol{K}_i)^{\mathrm{T}}\boldsymbol{X}_i + \boldsymbol{X}_i(\boldsymbol{A}_i + \boldsymbol{B}_{i2}\boldsymbol{K}_i) & \boldsymbol{X}_i\boldsymbol{B}_{i1} & \boldsymbol{C}_i^{\mathrm{T}} \\ \boldsymbol{B}_{i1}^{\mathrm{T}}\boldsymbol{X}_i & -\gamma_i^2\boldsymbol{I} & 0 \\ \boldsymbol{C}_i & 0 & -\boldsymbol{I}\end{bmatrix} < 0 \quad (68)$$

By (66), (64.4) and (60), we can obtain v_i. The adaptive law is expressed by (61).

Proof

For (65), when $y_i = \boldsymbol{C}_i\boldsymbol{Z}_i$ and the state feedback control law is $\bar{v}_{i1} = \boldsymbol{K}_i\boldsymbol{Z}_i$, we obtain

$$\dot{\boldsymbol{Z}}_i = (\boldsymbol{A}_i + \boldsymbol{B}_{i2}\boldsymbol{K}_i)\boldsymbol{Z}_i + \boldsymbol{B}_{i1}\boldsymbol{\varepsilon}_i \quad (69.1)$$

$$\boldsymbol{y}_i = \boldsymbol{C}_i\boldsymbol{Z}_i \quad (69.2)$$

Based on the linear H_∞ theory, when $\|\boldsymbol{T}_{z_i\varepsilon_i}\|_\infty < \gamma$, for (69), the Riccati Inequality (70) should be satisfied. Meanwhile, the optimal control law $\bar{v}_{i2}$ and the worst disturbance $\boldsymbol{\varepsilon}$ are (71) and (72), respectively.

$$\boldsymbol{X}_i\boldsymbol{A}_i+\boldsymbol{A}_i^{\mathrm{T}}\boldsymbol{X}_i+\gamma_i^{-2}\boldsymbol{X}_i\boldsymbol{B}_{i1}\boldsymbol{B}_{i1}^{\mathrm{T}}\boldsymbol{X}_i-\mu^{-2}\boldsymbol{X}_i\boldsymbol{B}_{i2}\boldsymbol{B}_{i2}^{\mathrm{T}}\boldsymbol{X}_i+\boldsymbol{C}_i\boldsymbol{C}_i^{\mathrm{T}}<0 \tag{70}$$

$$\bar{v}_{i1}=\boldsymbol{K}_i\boldsymbol{Z}_i=-\frac{1}{2\mu^2}\boldsymbol{B}_{i2}^{\mathrm{T}}\boldsymbol{X}_i\boldsymbol{Z}_i \tag{71}$$

$$\boldsymbol{\varepsilon}_i=\frac{1}{\gamma_i^2}\boldsymbol{B}_{i1}^{\mathrm{T}}\boldsymbol{X}_i\boldsymbol{Z}_i \tag{72}$$

Where $\boldsymbol{X}_i$ is the positive define matrix; $\mu>0$.
Substituting (71) into (70), we obtain:

$$\boldsymbol{X}_i(\boldsymbol{A}_i+\boldsymbol{B}_{i2}\boldsymbol{K}_i)+(\boldsymbol{A}_i+\boldsymbol{B}_{i2}\boldsymbol{K}_i)^{\mathrm{T}}\boldsymbol{X}_i+\gamma_i^{-2}\boldsymbol{X}_i\boldsymbol{B}_{i1}\boldsymbol{B}_{i1}^{\mathrm{T}}\boldsymbol{X}_i+\boldsymbol{C}_i\boldsymbol{C}_i^{\mathrm{T}}<0 \tag{73}$$

By the Schur theorem, (73) can be rewritten as:

$$\begin{bmatrix}(\boldsymbol{A}_i+\boldsymbol{B}_{i2}\boldsymbol{K}_i)^{\mathrm{T}}\boldsymbol{X}_i+\boldsymbol{X}_i(\boldsymbol{A}_i+\boldsymbol{B}_{i2}\boldsymbol{K}_i) & \boldsymbol{X}_i\boldsymbol{B}_{i1} & \boldsymbol{C}_i^{\mathrm{T}}\\ \boldsymbol{B}_{i1}^{\mathrm{T}}\boldsymbol{X}_i & -\gamma_i^2\boldsymbol{I} & 0\\ \boldsymbol{C}_i & 0 & -\boldsymbol{I}\end{bmatrix}<0 \tag{74}$$

When the left right multiplying matrix of (74) is $diag\{\boldsymbol{X}_i^{-1},\boldsymbol{I},\boldsymbol{I}\}$, we can obtain:

$$\begin{bmatrix}\boldsymbol{A}_i\boldsymbol{P}_i+\boldsymbol{B}_{i2}\boldsymbol{W}_i+(\boldsymbol{A}_i\boldsymbol{P}_i+\boldsymbol{B}_{i2}\boldsymbol{W}_i)^{\mathrm{T}} & \boldsymbol{B}_{i1} & \boldsymbol{P}_i\boldsymbol{C}_i^{\mathrm{T}}\\ \boldsymbol{B}_{i1}^{\mathrm{T}} & -\gamma_i^2\boldsymbol{I} & 0\\ \boldsymbol{C}_i\boldsymbol{P}_i & 0 & -\boldsymbol{I}\end{bmatrix}<0 \tag{75}$$

Where $\boldsymbol{P}_i=\boldsymbol{X}_i^{-1}$ is the positive define matrix; $\boldsymbol{K}_i=\boldsymbol{W}_i\boldsymbol{P}_i^{-1}$。

By the **Mincx** command in Matlab, the minimum value of γ_i and the values of $\boldsymbol{W}_i$ and $\boldsymbol{P}_i$ can be resolved. So the OP-L2-RADEC can be realized by (66), (64.4), (60) and (61).

Remark 6

The OP-L2-RAEC can not only improve system robustness to disturbances and be adaptive to the dynamic uncertainties, but also can be applied to minimize the impact of disturbance by solving the linear matrix inequality to obtain the optimal control law.

Remark 7

In C-L2-RADEC and K-L2-RADEC, the control law and the adaptive law are:

$$v_i=-\frac{e_{i2}e_{i3}}{b_{i2}}-\varphi_{i3}\hat{\theta}_{i2}+m_{i1}(e_{i1}-m_{i2}x_{i2})-e_{i2}+\dot{\hat{\theta}}_{i1}x_{i2}-(-\hat{\theta}_{i1}+m_{i1}+m_{i2})(-\hat{\theta}_{i1}x_{i2}+x_{i3})-m_{i3}b_{i2}-u_{if1}$$, $$\dot{\hat{\theta}}_{i1}=-\rho_{i1}\left[x_{i2}e_{i2}+(-\hat{\theta}_{i1}+m_{i1}+m_{i2})x_{i2}b_{i2}\right]$$,

$$\dot{\hat{\theta}}_{i2}=\rho_{i2}b_{i2}\varphi_{i3}$$.

In OP-L2-RADEC, the control law and the adaptive law are:

$$\bar{v}_{i1}=\boldsymbol{W}_i\boldsymbol{P}_i^{-1}\boldsymbol{Z}_i$$, $$u_{if1}=(m_{i1}^2+m_{i2}^2+m_{i1}m_{i2}-2)e_{i2}-\bar{v}_{i1}-(m_{i1}+m_{i2}+m_{i3})e_{i3}+\dot{\hat{\theta}}_i x_{i2}$$,

$$v_i=\frac{\omega_0}{2H_i}\left[-\frac{I_{iq}}{T'_{d0i}}E_{fi}+\frac{1}{T'_{d0i}}P_{ei}-E'_{iq}\dot{I}_{iq}\right]$$, $$v_i=-\frac{e_{i2}e_{i3}}{b_{i2}}-\varphi_{i3}\hat{\theta}_{i2}+m_{i1}(e_{i1}-m_{i2}x_{i2})-e_{i2}+\dot{\hat{\theta}}_{i1}x_{i2}-(-\hat{\theta}_{i1}+m_{i1}+m_{i2})(-\hat{\theta}_{i1}x_{i2}+x_{i3})-m_{i3}b_{i2}-u_{if1}$$,

$$\dot{\hat{\theta}}_{i1}=\rho_{i1}\left[-x_{i2}e_{i2}-(-\hat{\theta}_{i1}+m_{i1}+m_{i2})x_{i2}e_{i3}\right]$$, $$\dot{\hat{\theta}}_{i2}=\rho_{i2}e_{i3}\varphi_{i3}$$.

Where $e_{i1} = \Delta\delta_i$, $e_{i2} = \Delta\omega_i + m_{i1}\Delta\delta_i$, $e_{i3} = x_{i3} + e_{i1} - \hat{\theta}_i x_{i2} + m_{i1}x_{i2} + m_{i2}e_{i2}$, $x_{i3} = P_{ie0} - P_{ie}$, $E'_{qi} \approx V_{ti} + \frac{x'_{di}Q_{ei}}{V_{ti}}$, $\boldsymbol{z}_i = [z_{i1} \ z_{i2} \ z_{i3}]^{\mathrm{T}}$, $z_{i1} = \Delta\delta_i$, $z_{i2} = \Delta\omega_i$, $z_{i3} = \Delta\dot{\omega}_i$.

In above mentioned control law and adaptive law of the generator *i*, all the variables and parameters are just related to the same generator, so it is clear that C-L2-RADEC, K-L2-RADEC and OP-L2-RADEC are all decentralized control.

In C-L2-RADEC, K-L2-RADEC and OP-L2-RADEC, it is necessary to obtain the values of $I_{i\mathrm{q}}$, $I_{i\mathrm{d}}$ and $\dot{I}_{i\mathrm{q}}$. In this paper, these state values of the generator are estimated by EKF that is introduced in Section 3.4.

3.4. State Variable EKF Estimate of Generator

The relation between the rotor speed ω_i and the rotor position $\bar{\theta}_i$ of the *i*th generator is:

$$\dot{\bar{\theta}}_i = \omega_i \tag{76}$$

For the high sampling frequency in the excitation control system, the rotor speed can be assumed to be constant in the sampling period, *i.e.*

$$\dot{\omega}_i = 0 \tag{77}$$

In the d, q reference coordinate system, the flux linkage equation of the *i*th synchronous generator can be described as

$$\dot{\boldsymbol{\varphi}}_{i\delta\mathrm{d}} = \boldsymbol{u}_{i\mathrm{d}} + \boldsymbol{R}_i \boldsymbol{i}_{i\mathrm{d}} + \boldsymbol{\omega}_i \boldsymbol{\varphi}_{i\delta\mathrm{q}} \tag{78}$$

$$\dot{\boldsymbol{\varphi}}_{i\delta\mathrm{q}} = \boldsymbol{u}_{i\mathrm{q}} + \boldsymbol{R}_i \boldsymbol{i}_{i\mathrm{q}} - \boldsymbol{\omega}_i \boldsymbol{\varphi}_{i\delta\mathrm{d}} \tag{79}$$

$$\varphi_{i\delta\mathrm{q}} = \varphi_{i\mathrm{aq}} = L_{i\mathrm{q}} i_{i\mathrm{q}} \tag{80}$$

$$\varphi_{i\delta\mathrm{d}} = \varphi_{i\mathrm{ad}} + \varphi_{i\mathrm{f}} = L_{i\mathrm{d}} i_{i\mathrm{d}} + \varphi_{i\mathrm{f}} \tag{81}$$

$$\dot{\boldsymbol{\varphi}}_{i\delta} = \dot{\boldsymbol{\varphi}}_{i\delta\mathrm{d}} + \dot{\boldsymbol{\varphi}}_{i\delta\mathrm{q}} \tag{82}$$

Where $u_{i\mathrm{d}}$, $u_{i\mathrm{q}}$, $i_{i\mathrm{d}}$, $i_{i\mathrm{q}}$ are the d-q axis stator voltages and currents, respectively; R_i is the stator resistance; $L_{i\mathrm{d}}$, $L_{i\mathrm{q}}$ are the d-q axis stator inductances; $\varphi_{i\mathrm{d}}$, $\varphi_{i\mathrm{q}}$ are the d-q axis stator flux linkage, respectively; $\varphi_{i\mathrm{f}}$ is the rotor flux linkage.

From (78)-(82), the synchronous generator can be described by (83).

$$\begin{aligned} \dot{\boldsymbol{x}} &= \boldsymbol{f}(x) + \boldsymbol{B}(x)\boldsymbol{U} \\ \boldsymbol{y} &= [i_{\mathrm{D}} \ \ i_{\mathrm{Q}}]^{\mathrm{T}} = \boldsymbol{h}(\boldsymbol{x}) \end{aligned} \tag{83}$$

Where $\boldsymbol{x} = [x_1 \ x_2 \ x_3 \ x_4]^{\mathrm{T}} = [\varphi_{i\delta\mathrm{d}} \ \ \varphi_{i\delta\mathrm{q}} \ \ \bar{\theta}_i \ \ \omega_i]^{\mathrm{T}}$, $\begin{bmatrix} i_{i\mathrm{D}} \\ i_{i\mathrm{Q}} \end{bmatrix} = \sqrt{\frac{2}{3}} \begin{bmatrix} 1 & -\frac{1}{2} & -\frac{1}{2} \\ 0 & \frac{\sqrt{3}}{2} & -\frac{\sqrt{3}}{2} \end{bmatrix} \begin{bmatrix} i_{i\mathrm{a}} \\ i_{i\mathrm{b}} \\ i_{i\mathrm{c}} \end{bmatrix}$,

$\begin{bmatrix} u_{i\mathrm{D}} \\ u_{i\mathrm{Q}} \end{bmatrix} = \sqrt{\frac{2}{3}} \begin{bmatrix} 1 & -\frac{1}{2} & -\frac{1}{2} \\ 0 & \frac{\sqrt{3}}{2} & -\frac{\sqrt{3}}{2} \end{bmatrix} \begin{bmatrix} u_{i\mathrm{a}} \\ u_{i\mathrm{b}} \\ u_{i\mathrm{c}} \end{bmatrix}$, $\begin{bmatrix} i_{\mathrm{d}} \\ i_{\mathrm{q}} \end{bmatrix} = \begin{bmatrix} \cos\bar{\theta} & -\sin\bar{\theta} \\ \sin\bar{\theta} & \cos\bar{\theta} \end{bmatrix} \begin{bmatrix} i_{\mathrm{D}} \\ i_{\mathrm{Q}} \end{bmatrix}$, $\begin{bmatrix} u_{\mathrm{d}} \\ u_{\mathrm{q}} \end{bmatrix} = \begin{bmatrix} \cos\bar{\theta} & -\sin\bar{\theta} \\ \sin\bar{\theta} & \cos\bar{\theta} \end{bmatrix} \begin{bmatrix} u_{\mathrm{D}} \\ u_{\mathrm{Q}} \end{bmatrix}$,

$\boldsymbol{h}(\boldsymbol{x})=\begin{bmatrix}\frac{x_2}{x_{i\mathrm{q}}}\cos\bar{\theta}_i-\frac{x_1-\varphi_{i\mathrm{f}}}{x_{i\mathrm{d}}}\sin\bar{\theta}_i\\ \frac{x_2}{x_{i\mathrm{q}}}\sin\bar{\theta}_i-\frac{x_1-\varphi_{i\mathrm{f}}}{x_{i\mathrm{d}}}\cos\bar{\theta}_i\end{bmatrix}$, $\boldsymbol{B}(x)=\begin{bmatrix}\cos\bar{\theta}_i & -\sin\bar{\theta}_i\\ \sin\bar{\theta}_i & \cos\bar{\theta}_i\end{bmatrix}$, $U=[u_{i\mathrm{D}}\ \ u_{i\mathrm{Q}}]^{\mathrm{T}}$,
$\boldsymbol{f}(\boldsymbol{x})=\begin{bmatrix}\frac{R_i}{x_{i\mathrm{d}}}x_1+x_2x_4-\frac{R_i}{x_{i\mathrm{d}}}\varphi_{i\mathrm{f}} & \frac{R_i}{x_{i\mathrm{q}}}x_2-x_1x_4 & x_4 & 0\end{bmatrix}^{\mathrm{T}}$, i_{ia}, i_{ib}, i_{ic}, u_{ia}, u_{ib} and u_{ic} are instantaneous current and voltage values of the ith generator.

For the fully digital implementation, the system model (83) can be re-written as:

$$\begin{aligned}\boldsymbol{x}_{k+1}&=\boldsymbol{F}_d(x_k)x_k+\boldsymbol{D}(x_k)\boldsymbol{u}_k+\boldsymbol{V}_k\\ \boldsymbol{y}_k&=\boldsymbol{h}(\boldsymbol{x}_k)\boldsymbol{x}_k+\boldsymbol{W}_k\end{aligned}\tag{84}$$

Where $\boldsymbol{V}_k$ and $\boldsymbol{W}_k$ are the zero-mean Gaussian random vectors, describing the model disturbance and the measurement disturbance, whose variance matrices are $\boldsymbol{Q}$ and $\boldsymbol{R}$, respectively, $\boldsymbol{F}_d(x_k)=1+T_{\mathrm{c}}\boldsymbol{f}(\boldsymbol{x}(kT_{\mathrm{c}}))$, $\boldsymbol{D}(x_k)=1+T_{\mathrm{c}}B(\boldsymbol{x}(kT_{\mathrm{c}}))$, T_{c} is the sampling period.

$\boldsymbol{x}_{k+1}$ can be estimated by EKF in following two steps.

Step 1: Prediction step

$\tilde{\boldsymbol{x}}_{k+1}=\boldsymbol{F}(\tilde{x}_k)\tilde{x}_k+\boldsymbol{D}(\tilde{x}_k)\boldsymbol{u}_k$; $\tilde{\boldsymbol{y}}_{k+1}=\boldsymbol{h}(\tilde{\boldsymbol{x}}_{k+1})\tilde{\boldsymbol{x}}_{k+1}$; $\tilde{\boldsymbol{P}}_{k+1}=\boldsymbol{P}_k+T_{\mathrm{c}}\{\boldsymbol{F}_k\boldsymbol{P}_k+\boldsymbol{P}_k\boldsymbol{F}_k^{\mathrm{T}})\}+\boldsymbol{Q}$

Step 2: Innovation step

$\boldsymbol{K}_{k+1}=\tilde{\boldsymbol{P}}_{k+1}\boldsymbol{H}_{k+1}^{\mathrm{T}}[\boldsymbol{H}_{k+1}\tilde{\boldsymbol{P}}_{k+1}\boldsymbol{H}_{k+1}^{\mathrm{T}}+\boldsymbol{R}]^{-1}$; $\boldsymbol{x}_{k+1}=\tilde{\boldsymbol{x}}_{k+1}+K_{k+1}[\boldsymbol{y}_{k+1}-\tilde{\boldsymbol{y}}_{k+1}]$; $\boldsymbol{P}_{k+1}=\tilde{\boldsymbol{P}}_{k+1}-\boldsymbol{K}_{k+1}\boldsymbol{H}_{k+1}\tilde{\boldsymbol{P}}_{k+1}$

Where $\boldsymbol{F}_k=\frac{\partial\boldsymbol{f}(\boldsymbol{x})}{\partial\boldsymbol{x}}|_{\boldsymbol{x}=\boldsymbol{x}_k}$, $\boldsymbol{H}_k=\frac{\partial\boldsymbol{h}(\boldsymbol{x})}{\partial\boldsymbol{x}}\Big|_{\boldsymbol{x}=\boldsymbol{x}_k}$ are the Jacobian matrix.

The values of $I_{i\mathrm{q}}$ and $I_{i\mathrm{d}}$ by $\begin{bmatrix}I_{i\mathrm{d}}\\ I_{i\mathrm{q}}\end{bmatrix}=\begin{bmatrix}\cos\bar{\theta}_i & -\sin\bar{\theta}_i\\ \sin\bar{\theta}_i & \cos\bar{\theta}_i\end{bmatrix}\begin{bmatrix}i_{i\mathrm{D}}\\ i_{i\mathrm{Q}}\end{bmatrix}$, The value of $\dot{I}_{i\mathrm{q}}$ can be obtained by $\dot{I}_{i\mathrm{q}}=(u_{i\mathrm{q}}+R_iI_{i\mathrm{q}}-\omega_i\varphi_{i\delta\mathrm{d}})/x_{\mathrm{q}}$.

Meanwhile, The value of $\boldsymbol{x}=[x_1\ \ x_2\ \ x_3\ \ x_4]^{\mathrm{T}}=[\varphi_{i\delta\mathrm{d}}\ \ \varphi_{i\delta\mathrm{q}}\ \ \bar{\theta}_i\ \ \omega_i]^{\mathrm{T}}$ can be estimated by EKF.

3.5. L2- RADEC Based on Sensor-less State Tracking Estimation

For the ith generator, the block diagram of C-L2-RADEC, K-L2-RADEC and OP-L2-RADEC based on the state estimate is shown in Figure 1.

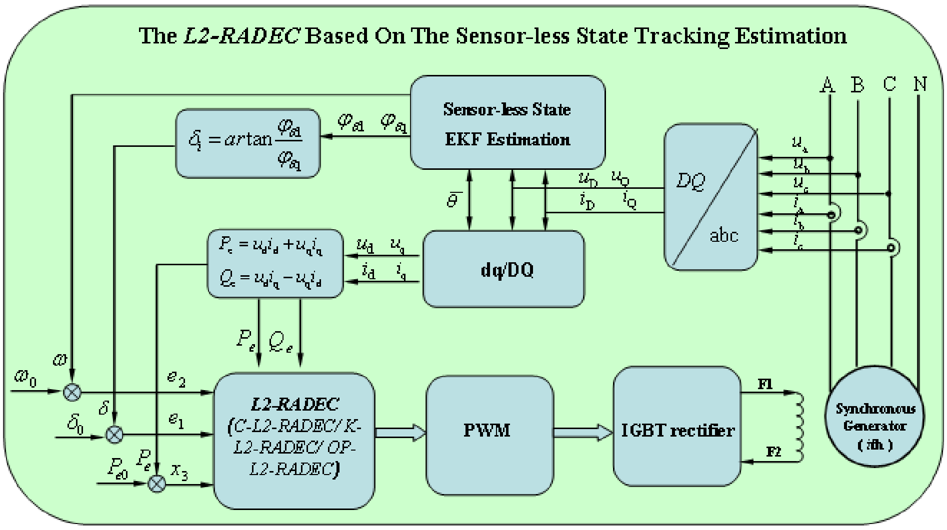

Figure 1. Block Diagram of L2-RADEC Based on Sensor-less State Tracking Estimation

In Figure 1, the values of $\varphi_{i\delta d}$, $\varphi_{i\delta q}$ and $\bar{\theta}_i$ can be obtained by the EKF estimate. By $\delta_i = \frac{\varphi_{i\delta d}}{\varphi_{i\delta q}}$, e_{i1} can be calculated. u_{iD}, u_{iQ}, i_{iD} and i_{iQ} can be obtained by the 3/2 transformation of stator voltage and stator current (introduced in Section 3.4). u_{id}, u_{iq}, i_{id}, i_{iq} can be obtained by the DQ/dq transformation of u_{iD}, u_{iQ}, i_{iD}, i_{iQ} (introduced in Section 3.4). By $P_e = u_d i_d + u_q i_q$, $Q_e = u_d i_q - u_q i_d$, $x_{i3} = P_{ie0} - P_{ie}$, $E'_{qi} \approx V_{ti} + x'_{di} Q_{ei} / V_{ti}$, $\dot{i}_{iq} = (u_{iq} + R_i i_{iq} - \omega_i \varphi_{i\delta d}) / L_{iq}$, the values of e_{i1}, e_{i2}, e_{i3}, x_{i3}, E'_{qi}, I_{iq}, I_{id} and $\dot{i}_{iq}$ can be obtained and the OP-L2-RAEC can be realized (introduced in Section 3.3 and Section 3.4).

4. Simulation and Experiment

Simulation has been conducted on a 4-machine power system (see Figure 2).

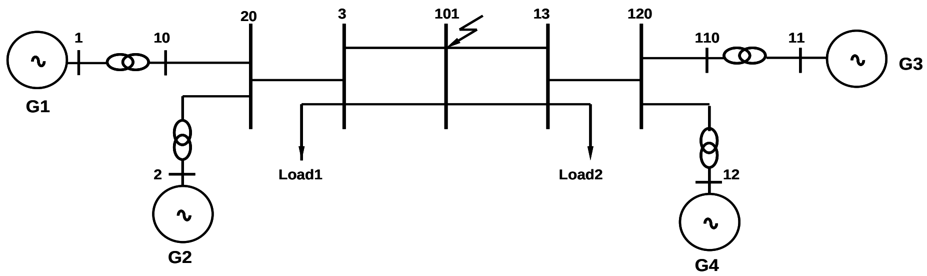

Figure 2. Diagram of the 4-Machine Power System

The system data is listed in Appendix A. In the simulation, the models of generators are same as (4) and the governor dynamic are neglected. The loads are represented by constant impedances. The value of the uncertain parameter is given as D= 3p.u.~ 5p.u.. Parameters of AVR+PSS controllers are list in Appendix B.

4.1. Simulation on State Variables Estimate by EKF

When there are the Gaussian white noise in System (83) and the loads of the 2th generator increase by 50% at 2.5 s, the actual, estimated values and the values with noise of $\varphi_{2\delta d}$, $\varphi_{2\delta q}$ and $\bar{\theta}_2$ of the 2th generator are shown in Figure 3. The EKF program is list in Appendix C.

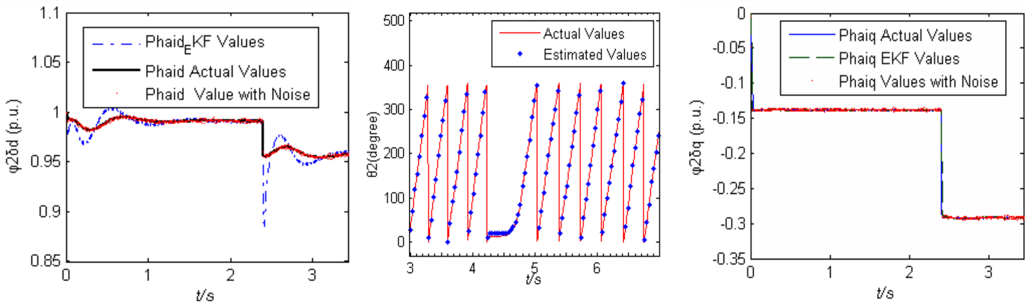

(a) $\varphi_{2\delta d}$ (b) $\bar{\theta}_2$ (c) $\varphi_{2\delta q}$

Figure 3. Comparison between Actual Values and Estimated Values

As shown in Figure 3, although the transient estimated derivate the actual values, the estimated values will be convergent to the actual value. In the steady state, the values of the errors between the actual values and the estimated values are small, so the values of $\varphi_{\delta q}$, $\varphi_{\delta d}$ and $\bar{\theta}_2$ can be estimated accurately by EKF. So the values of $\delta = ar\tan\frac{\varphi_{\delta d}}{\varphi_{\delta q}}$, e_{i1}, e_{i2}, e_{i3}, x_{i3}, E'_{qi}, I_{iq}, I_{id} and $\dot{I}_{iq}$ can be obtained, and C-L2-RADEC, K-L2-RADEC and OP-L2- RADEC can be realized.

4.2. Comparison between C-L2-RADEC, K-L2-RADEC, OP-L2-RADEC and AVR+PSS

The 3-phase short fault happens on line 3-101 close to 101 at 5.3 s and the fault line trips at 5.4 s. When the auto voltage regulator and power system stabilizer (AVR+PSS) are all adopted, the state parameter dynamic curves of the power system are shown in Figure 4.

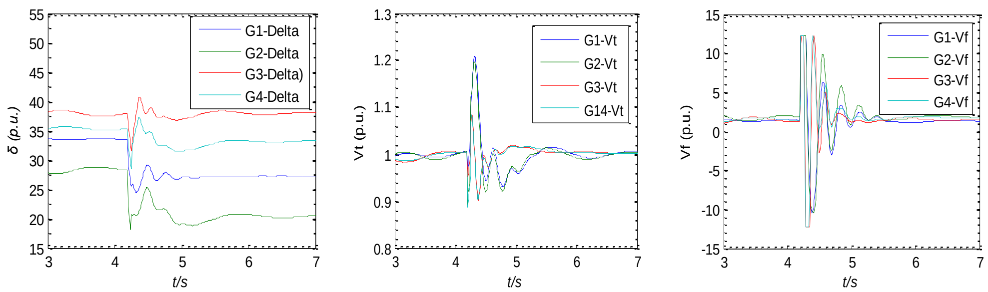

(a) Power Angle (b) Terminal Voltage (c) Excitation Voltage

Figure 4. Dynamic Curves of Generator State Variables by AVR+PSS Control

When the C-L2-RADEC is adopted and $m_{i1} = m_{i2} = m_{i3} = 1$, $\gamma_i = 2$, $\rho_{i1} = \rho_{i2} = 1$ and $f(e_{i3}) = 2e_{i3} + 1$, the state parameter dynamic curves of the generators are shown in Figure 5.

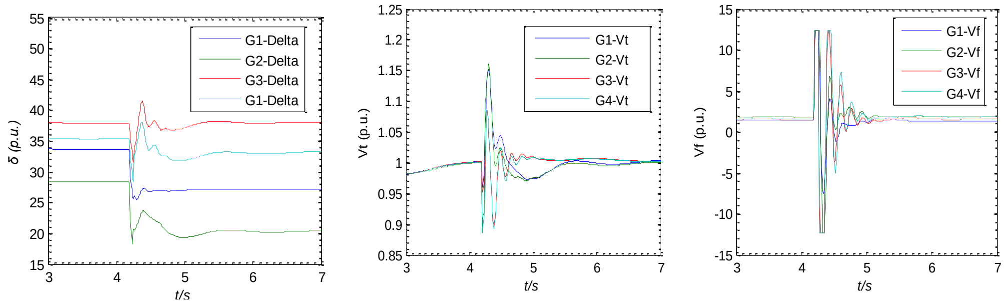

(a) Power Angle (b) Terminal Voltage (c) Excitation Voltage

Figure 5. State Parameter Curves of Generators by C-L2-RADEC

As shown in Figure 4 and Figure 5, when 3-phase short fault happens suddenly, comparing with the AVR+PSS control, the C-L2-RADEC can improve the convergence rate of the state parameters. At the same time, because the damp constant D is uncertain, Figure 5 shows that C-L2-RADEC can effectively increase robust performance of the uncertain excitation system.

When $c_{i1} = c_{i2} = c_{i3} = 1$, $f_{i1}(|e_{i1}|) = e_{i1}^2$, $f_{i2}(|e_{i2}|) = 4e_{i2}^2$, $f_{i3}(|e_{i3}|) = 5e_{i3}^4$, $\rho_{i1} = \rho_{i2} = 1$, $\gamma_i = 2$ and $f(e_{i3}) = 2e_{i3} + 1$, adopting K-L2-RADEC, state parameter dynamic curves are shown in Figure 6.

As shown in Figure 5 and Figure 6, When the value of e_{ij} is bigger, the values of m_j will increases, so the convergence speed of state parameters will be improved.

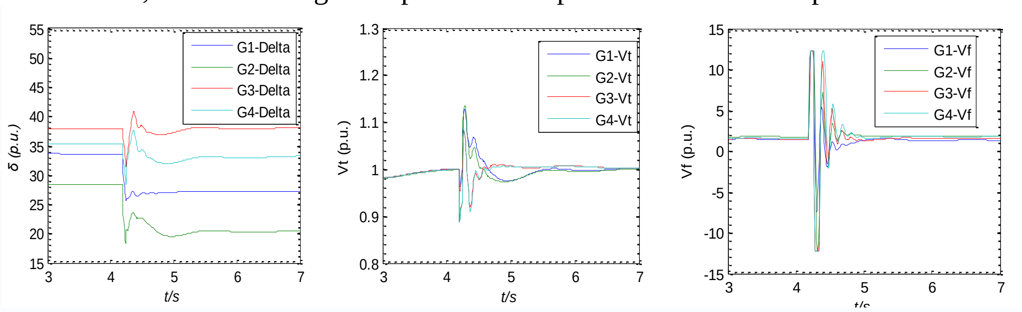

(a) Power Angle (b) Terminal Voltage (c) Excitation Voltage

Figure 6. State Parameter Curves of Generators by K-L2-RADEC

When $y_i = \boldsymbol{C}_i \boldsymbol{Z}_i$, $\boldsymbol{C}_i = \text{diag}[1, 0.4, 0.1]$, $m_{i1} = 2, m_{i2} = 1, m_{i3} = 4$, $\gamma_i = 2$, the LMI (75) can be resolved by the function Mincx in MATLAB LMI toolbox, we can get $\boldsymbol{P}_i = \begin{bmatrix} 1.7393 & -0.9851 & 0.5378 \\ -0.9851 & 2.4947 & 0.3604 \\ 0.5378 & 0.3604 & 3.1088 \end{bmatrix}$ and $\boldsymbol{W}_i = [10.0596 \ \ -2.9216 \ \ -2.1802]$. From (66) and (67), the optimal robust control law $\bar{v}_i$ and the worst disturbances ε_i are respectively as follows:

$$\bar{v}_i = 7.7546 z_{i1} + 2.2234 z_{i2} - 2.3005 z_{i3} = 7.7546(\delta - \delta_0) + 2.2234(\omega - \omega_0) - 2.3005\dot{\omega} \quad (85)$$

$$\varepsilon_i = \begin{bmatrix} 0.2463 & -0.6237 & -0.0901 \\ 0.1345 & 0.0901 & 0.7772 \end{bmatrix} \begin{bmatrix} \delta - \delta_0 \\ \omega - \omega_0 \\ \dot{\omega} \end{bmatrix} \quad (86)$$

Substituting (85) into (66), (60), we can get the control input v_i. The adaptive law is expressed by (61). The curves of the state parameters are shown in Figure 7.

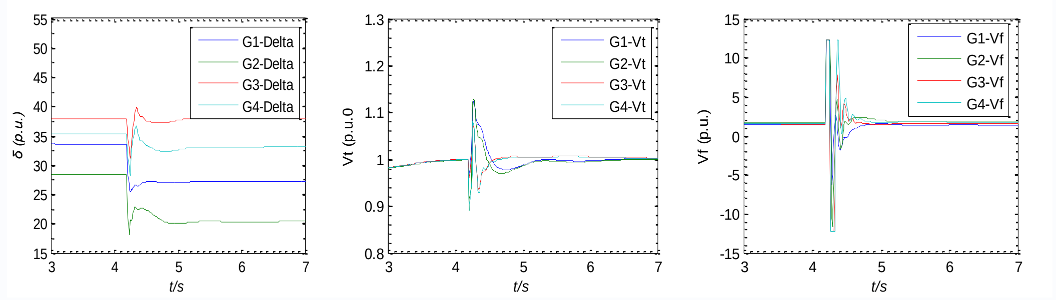

(a) Power Angle (b) Terminal Voltage (c) Excitation Voltage

Figure 7. State Parameter Curves of Generators by OP-L2-NRADEC

As shown in Figure 4, Figure 6 and Figure 7, when 3-phase short fault happens suddenly, comparing with the AVR+PSS control, the OP-L2-RADEC can improve the convergence rate of the state parameters. The OP-L2-RADEC can not only suppress the disturbance, stabilize the excitation system, be adaptive to the uncertain parameter, but also realize the optimal L2-gain disturbance attenuation.

5. Conclusion

New nonlinear robust adaptive L2-Ggain decentralized excitation controllers (C-L2-RADEC, K-L2-RADEC and OP-L2-RADEC) are proposed in this paper. Because the K-class functions are applied and the universal calculation formulae are deduced, the new controller can improve the convergence speed of the state parameters and overcome the over-parameterized problem in some robust adaptive excitation controller. In the new controllers, the values of state parameters are estimated by EKF. Simulations on the 4-machine power system demonstrate that comparing with the AVR+PSS control, the new excitation controllers are all robust to external disturbance and adaptive to the uncertain parameters and OP-L2- RADEC can realize the optimal L2 gain control to minimize the effect of the disturbance. Meanwhile, the values of state parameters can be estimated by EKF.

Appendix

Appendix A. Parameters of Generators and Transmission Lines

Table 1. Parameters of Generators

Parameters	Generator #1	Generator #2	Generator #3	Generator #4
x_{d}	1.8	1.65	1.2	0.93
x'_{d}	0.3	0.25	0.16	0.66
x_{q}	1.6	1.4	1.0	0.51
T'_{d0}	5.2	6.4	8.3	5.69
M	9.0	10.2	11.2	14.3

Table 2. Parameters of Transmission Lines

Bus	R(p.u.)	L(p.u.)	C(p.u.)	Bus	R(p.u.)	L(p.u.)	C(p.u.)
1-10	0	0.15	0	101-18	0.0043	0.0475	0.7802
2-20	0	0.10	0	18-120	0.0003	0.0059	0.0680
10-20	0.0010	0.025	00.75	120-110	0.0010	0.025	00.75
20-8	0.0003	0.0059	0.0680	120-12	0	0.10	0
8-101	0.0043	0.0475	0.7802	110-11	0	0.15	0

Appendix B. PSS Transfer Function

Generator 1:

$$G_1(s)=\frac{30}{0.015s+1}\frac{0.05s+1}{0.02s+1}\frac{3s+1}{5.4s+1}$$

Generator 2:

$$G_2(s)=\frac{21}{0.015s+1}\frac{0.03s+1}{0.015s+1}\frac{2.4s+1}{3.2s+1}$$

Generator 3:

$$G_3(s)=\frac{43}{0.015s+1}\frac{0.06s+1}{0.042s+1}\frac{3.4s+1}{4.2s+1}$$

Generator 4:

$$G_4(s)=\frac{50}{0.015s+1}\frac{0.34s+1}{0.126s+1}\frac{3s+1}{3.2s+1}$$

Appendix C. EKF Program

```
syms phaid phaiq theta w
x=[phaid;phaiq;theta]
Q=10*eye(3)
P=10*eye(3)
RR=10*eye(2)
xinitial=[1;0;0]
for i=1:1:(dimension/substract_step)
phaidEKFplot(i)=xinitial(1);
phaiqEKFplot(i)=xinitial(2);
thetaEKFplot(i)=xinitial(3);
Fx=120*pi*[(-R/L1*phaid+phaiq*wEKF(i)+R/L1*(phaimdEKF(i)-ikdEKF(i)));(-R/L1*phaiq-
phaid*wEKF(i)+R/L1*(phaimqEKF(i)-ikqEKF(i)));wEKF(i)]
Fd=[phaid;phaiq;theta]+tc*Fx
B=[1 0;0 1;0 0];
D=120*pi*tc*B
Hx=[(-phaid+phaimdEKF(i)-ikdEKF(i))/L1;(-phaiq+phaimqEKF(i)-ikqEKF(i))/L1]
xkadd1=Fd+D*[udEKF(i);uqEKF(i)];
Fjacobi=jacobian(Fd,[phaid phaiq theta])
Hjacobi=jacobian(Hx,[phaid phaiq theta])
x=xinitial
xkadd1Pred=subs(xkadd1,[phaid phaiq theta],x)
yk=[(-xkadd1Pred(1)+phaimdEKF(i)-ikdEKF(i))/L1;(-xkadd1Pred(2)+phaimqEKF(i)-
ikqEKF(i))/L1];
F=subs(Fjacobi,[phaid phaiq theta],x)
P=Q+F*P*F'
H=subs(Hjacobi,[phaid phaiq theta],x)
KKadd1=P*H'*inv(H*P*H'+RR)
xinitial=xkadd1Pred+KKadd1*[idEKF(i)-yk(1);iqEKF(i)-yk(2)]
P=P-KKadd1*H*P
```

Acknowledgments

This research is financially supported by National Natural Science Foundation of China (Grant No. 51407196).

References

[1] Z.-F. Gu, C.-Q. Zhu and Shao Tianzhang, “Study on the AC tracking excitation based on the sensor-less air-gap field oriented technology”, Electric Power Automatic Equipment, vol. 10, no. 3, **(2011)**, pp. 52–56.

[2] Z.-F. Gu, C.-Q. Zhu and T.-Z. Shao, “Robust Adaptive Control for the Excitation System Based on Total-State-Parameter Optimal Control”, Control Theory & Applications, vol. 30, no. 7, **(2013)**, pp. 56-862.

[3] C. Yan, G. K. V. and K. Corzine, “Hardware implementation of an AIS-Based optimal excitation controller for an electric ship”, IEEE Transactions on Industry Applications, vol. 47, no. 2, **(2013)**, pp. 1060–1070.

[4] D.-Q. Gan , Z.-H. Qu and H.-Z. Cai , “Multi machine power system excitation control design via theories of feedback linearization control and nonlinear robust control”, International Journal of Systems Science, vol. 31, no. 4, **(2000)**, pp. 519–527.

[5] L. Cong, Y. Wang and D. J., “Coordinated control design of generator excitation and SVC for transient stability and voltage regulation enhancement of multi-machine power systems”, International Journal of Robust and Nonlinear Control, vol. 14, no. 9, **(2004)**, pp. 789–805.

[6] Q. Lu, Y. Sun, Z. Xu and T. Mochizuki, “Decentralized nonlinear optimal excitation control”, IEEE Transactions on Power Systems, vol. 11, no. 4, **(1996)**, pp. 957–1962.

[7] T. Hiyama, Y. Ueki and H. Andou, “Integrated fuzzy logic generator controller for stability enhancement”, IEEE Transactions on Energy Conversion, vol. 12, no. 4, **(1997)**, pp. 400–406.

[8] Y. Hsu and L. Chen, “Tuning of power system stabilizers using an artificial neural network”, Transactions on Energy Conversion, vol. 4, no. 6, **(1991)**, pp. 612–619.

[9] Y. Guo, D. J. Hill and Y. Wang, "Global transient stability and voltage regulation for power systems", IEEE Trans. Power Systems, vol. 16, no. 4, **(2001)**, pp. 678-688.
[10] J. W. Chapman, M. D. Ilic and C. A. King, "Stabilizing a multi machine power system via decentralized feedback linearizing excitation control", IEEE Trans. Power Systems, vol. 8, no. 3, **(1993)**, pp. 830–839.
[11] J. Hao, C. Chen, L. Shi and J. Wang, "Nonlinear decentralized disturbance attenuation excitation control for power systems with nonlinear loads based on the Hamiltonian theory", IEEE Trans. Energy Conversion, vol. 22, no. 2, **(2007)**, pp. 316–324.
[12] Y. Z. Wang, C. W. Li and D. Z. Cheng, "New approaches to generalized Hamiltonian realization of autonomous nonlinear systems", Science in China(Series F), vol. 46, no. 6, **(2003)**, pp. 431–444.
[13] G. L.v Alexander and M. José, "High-order block sliding-mode controller for a synchronous generator with an exciter system", IEEE Transactions on Industrial Electronics, vol. 58, no. 1, **(2011)**, pp. 337-347.
[14] Q. Lu, S. Mei and W. Hul, "Nonlinear decentralized disturbance attenuation excitation control via new recursive design for multi machine power systems", IEEE Trans. Power Systems, vol. 16, no. 4, **(2001)**, pp. 729-736.
[15] M. M. Polycarpou and P. A. Ioannou, "A robust adaptive nonlinear control design", Automatica, vol. 32, no. 3, **(1996)**, pp. 423-427.
[16] R. Marino and P. Tomei, "Robust adaptive state-feedback tracking for nonlinear systems", IEEE Trans. Automatic Control, vol. 43, no. 1, **(1998)**, pp. 84-89, 1998.
[17] Z.-P. Jiang and D. J. Hill, "A robust adaptive back-stepping scheme for nonlinear systems with un-modeled dynamics", IEEE Transactions on Automatic Control, vol. 44, no. 9, **(1999)**, pp. 1705-1711.
[18] Z.-F. Gu, C.-Q. Zhu and W.-J. Zhao, "AC tracking L2 excitation control based on the state estimation by EKF", Electric Machine and Control, vol. 1, no. 7, **(2013)**, pp. 11-19.
[19] K. Wang, H. Xin, D. Gan and Y. Ni, "Nonlinear robust adaptive excitation controller design in power systems based on a new back-stepping method", IET Control Theory and Applications, vol. 4, no. 12, **(2010)**, pp. 2947–2957.
[20] L. Qiang, S.-W. Mei and W. Hu, "Nonlinear decentralized disturbance attenuation excitation control via new recursive design for multi-machine power systems", IEEE Trans. Power Systems, vol. 16, no. 4, **(2001)**, pp. 729-736.
[21] G. Fusco and M. Russo, "Design of Decentralized Robust Controller for Voltage Regulation and Stabilization of Multimachine Power Systems", International Journal of Control, Automation, and Systems, vol. 11, no. 2, **(2013)**, pp. 277-285.
[22] Y.-Y. Wang, G.-X. Guo and D. J. Hill, "Robust decentralized nonlinear controller design for multi-machine power systems", Automatica, vol. 33, no. 9, **(1997)**, pp. 1725-1733.
[23] Q. Lu, S.-W. Mei and Y.-Z. Sun, "Nonlinear control of power systems", tsinghua press (Second edition), Beijing, **(2003)**.

Authors

Zhifeng Gu, He received the Ph.D. degree in Electrical Engineering from the Mechanical Engineering College, Shijiazhuang, China, in 2014. He is currently a lecture of the Mechanical Engineering College. His research interests include nonlinear robust control theory and application in stability control of isolated power system.

Changqing Zhu, He received the Ph.D. degree in Electro-technical Engineering from the Mechanical Engineering College, Shijiazhuang, China, in 2005. He is currently a professor of the Mechanical Engineering College. His research interests include power integrated theory and application in isolated power system.

Guixin Yang, she received the B.S. degree in Electrical Theory and New Technology from Hebei University of Technology, Tianjin, China, in 2006. She is currently a senior engineer of China Electronics Technology Corporation. Her research interests include stability control and power line communication of power system.

Wenting Wang, she received the B.S. degree in Electrical Engineering from Agriculture University of South China, Guangzhou, china, in 2005. She is currently a lecture of the Mechanical Engineering College. Her research interests include dynamic analysis and simulation of power system.

